

## CHAPTER 46

### Development of a Submerged Doppler-Type Directional Wave Meter

Tomotsuka Takayama<sup>1</sup>, Noriaki Hashimoto<sup>2</sup>, Toshihiko Nagai<sup>3</sup>  
Tomoharu Takahashi<sup>4</sup>, Hiroshi Sasaki<sup>5</sup>, and Yoshiki Ito<sup>6</sup>

#### Abstract

This paper presents a newly developed type of submerged directional wave meter having the capability to measure water surface elevation and multiple current velocity components. These components are determined from Doppler frequency shifts using the complex covariance method. The developed system was demonstrated to be capable of successfully obtaining directional wave data, as well as adequately estimating directional wave spectra.

#### 1. Introduction

Many types of wave observation devices have been developed over the years for various scientific and engineering applications. Most, however, were designed to measure only wave height and period, and consequently, a practical instrument incorporating features for satisfactorily measuring directional seas has not yet been obtained.

The most commonly used wave meter in Japan is a submerged ultrasonic-type wave gage that can be installed at a water depth of up to about 50 m. A submerged ultrasonic-type current meter developed for measuring directional seas, however, is limited to 30-m-deep water due to a decay of water particle velocity caused by waves. Obviously then, there is a need to develop a combined measuring system that can operate at 50 m.

---

<sup>1</sup> Director, Hydraulic Engineering Div., Port and Harbour Research Institute (PHRI),  
1-1 Nagase 3-chome, Yokosuka 239, Japan

<sup>2</sup> Chief, Ocean Energy Utilization Lab., Hydraulic Engineering Div., PHRI.

<sup>3</sup> Chief, Marine Observation Lab., Marine Hydrodynamics Div., PHRI.

<sup>4</sup> Managing Director, Japan Marine Surveyors Association,

14-12 Kodenma-cho, Nihonbashi, Chuo-ku, Tokyo 103, Japan

<sup>5</sup> Former manager, Measuring and Control System Div., Kaijyo Corporation,  
3-1-5 Sakae-cho, Hamura-shi, Tokyo 205, Japan

<sup>6</sup> Manager, Research and Development Div., Kaijyo Corporation.

This led to the present paper which describes a new device, named the submerged Doppler-type directional wave meter, that utilizes the Doppler effect of ultrasonic waves in water for measuring directional seas in coastal areas having a water depth of about 50 m.

## 2. Submerged Doppler-type directional wave meter

### 2.1 System description

**Figure 1** shows a circuit block diagram of the measurement system of the submerged Doppler-type directional wave meter. This system is comprised of a submerged transducer, measurement section, and computation unit. The measurement section consists of transceiver and signal processing circuits. The former circuit connects the transducer to the latter one which converts the signals to water surface elevation and current velocities after digitizing received analog quantities. The computation unit statistically analyzes wave data and computes the resultant directional wave spectra.

To measure the water surface elevation, the transducer radiates vertically-upward-directed ultrasonic waves ( $Z$ -axis, **Fig. 1**) and then receives the waves reflected off the water surface. The water surface elevation is estimated using the wave propagation time. By also radiating ultrasonic waves upward in four directions separated by an inclination angle  $\alpha$ , multiple current velocities are measured by receiving the waves scattered back from selected layers of water. The water particle velocity of each layer is estimated from the frequency shift caused by the Doppler

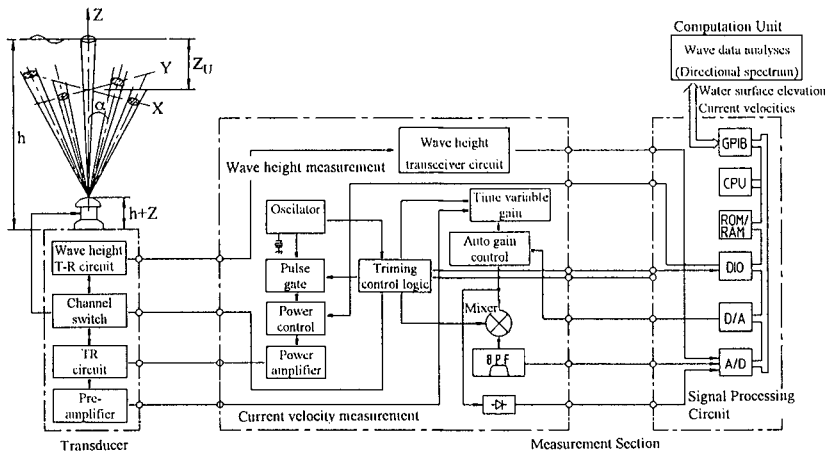


**Fig. 1** Diagram of the measurement system of the submerged Doppler-type directional wave meter.

**Table 1** Specifications of the Doppler-type directional wave meter.

Specification	Current Velocity	Wave Height
Measurement system	Ultrasonic Doppler method	Ultrasonic wave propagation time
Operating frequency	500 kHz	200 kHz
Beam width	1	30
Measurement channel	Orthogonal 4 channels	Vertical 1 channel
Beam tilt	300	—
Maximum output power	300 W	--
Measurement range	0 to $\pm 5$ m/s	0 ~ 30 m
Range resolution	2.3 m	—
Transmission interval	165 ms	165 ms
Measurement period	900 ms	495 ms

effect between the radiated and scattered waves. Use of a time sharing system enables all these measurements to be successively carried out at very short time intervals. Specifications of the new wave meter are summarized in **Table 1**.

## 2.2 Doppler frequency estimation methods

Two different techniques exist for conducting Doppler frequency analysis: (1) use of analog signals, such as the phase lock loop (PLL) or analog filter bank methods; and (2) use of digital signals, such as the fast Fourier transformation (FFT) and complex covariance (CC) methods. Of these, real-time processing is normally performed with the FFT or CC method due to rapid developments in microcomputers and peripheral equipment.

The FFT method has an advantage in that even at a low S/N ratio it can analyze the scattered wave signal to estimate the spectral density over the entire frequency band. At a higher S/N ratio, however, the CC method is more advantageous because computing the spectral moment is easier and the frequency resolution is better.

**Figure 2** shows a flow chart of the CC method's computational procedure, where the the input frequency signals  $\cos(\omega_{in}t + \epsilon)$  are first damped by the local oscillation frequency signals ( $\cos\omega_0t$  and  $\sin\omega_0t$ ) having a phase difference of  $90^\circ$ . Next, the first order moment  $\mu_1$  (average frequency) of the input signal is computed from the complex covariance function  $R(\tau)$  obtained from the outputs  $X_r(t_n)$  and  $X_i(t_n)$ . More specifically, the frequency components of  $\omega_{in} + \omega_0$  and  $\omega_{in} - \omega_0$  are obtained by mixing the input signals  $\cos(\omega_{in}t + \epsilon)$  with the cos and sin components of the local oscillation signals having frequency  $\omega_0$ . The difference component  $\omega_{in} - \omega_0$

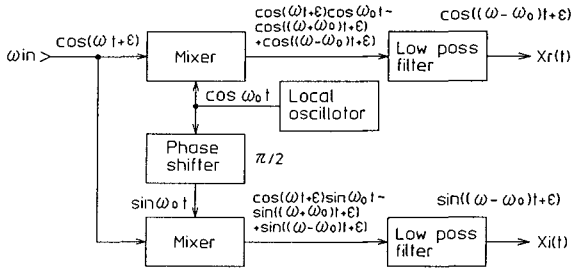


Fig. 2 Analog method for generating complex signals.

is then sent to a low pass filter (LPF) and A/D converter where it digitized. From  $X_r(t_n)$  and  $X_i(t_n)$ , the complex values  $Z(t_n)$  are obtained by  $Z(t_n) = X_r(t_n) + iX_i(t_n)$ , followed by computing  $\mu_1$  using

$$R(\tau) = \frac{1}{N} \sum_{n=1}^{N-1} Z(t_n)Z^*(t_n + \tau) \tag{1}$$

$$\mu_1 = \frac{1}{2\pi\tau} \tan^{-1} \frac{\text{Im}[R(\tau)]}{\text{Re}[R(\tau)]}, \tag{2}$$

where  $Z^*(t_n)$  is the complex conjugate of  $Z(t_n)$ .

This procedure can also be performed by the simple homodyne complex covariance (SHCC) method which simplifies the computation (Ito et al., 1989). Figure 3 shows a flow chart of this method's data processing procedure. Since the received signal is digitized, the sampling frequency  $f_s$  is easily synchronized with the transmitting wave which is four times larger than the transmitting frequency  $f_0$ . The reference signals for the homodyne detection can then be simulated as

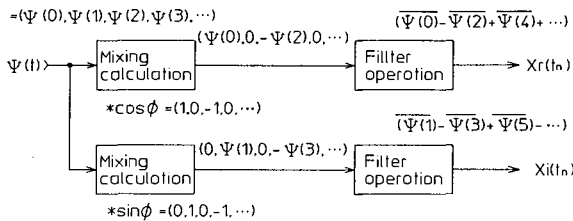


Fig. 3 Data processing for the SHCC method.

$$\begin{aligned}\cos \phi &= (1, 0, -1, 0, 1, 0, -1, \dots) \\ \sin \phi &= (0, 1, 0, -1, 0, 1, 0, \dots)\end{aligned}\quad (3)$$

Therefore, the outputs of homodyne circuit can be approximated by

$$\begin{aligned}\psi(t) \cos \phi &= \psi(0), 0, -\psi(2), 0, \psi(4), 0, \dots \\ \psi(t) \sin \phi &= 0, \psi(1), 0, -\psi(3), 0, \psi(5), \dots\end{aligned}\quad (4)$$

where  $\psi(t)$  is the received signal. If we utilize a LPF, by making block averages (16 points) of these series, the complex beat signal series,  $X_r(t)$  and  $X_i(t)$ , can be obtained. Then  $R(\tau)$  is subsequently determined by Eq. (1) and the Doppler or beat frequency  $\mu_1$  can be estimated as per the CC method (Eq. (2)).

When background noise is approximately stationary during a pulse repetition period, noise compensation can be accomplished using

$$\mu_1 = \frac{1}{2\pi\tau} \tan^{-1} \frac{\text{Im}[R(\tau)] - \text{Im}[R_n(\tau)]}{\text{Re}[R(\tau)] - \text{Re}[R_n(\tau)]}, \quad (5)$$

where  $R_n(\tau)$  indicates the complex covariance of the noise process.

Field experimental data shows this method estimates the current velocity at a S/N ratio corresponding to actual sea conditions with a mean error of about 2 to 6 cm/s and standard deviation of about 1 to 2 cm/s.

### 2.3 Analysis of directional spectrum

The extended maximum likelihood method (EMLM) developed by Isobe et al. (1984) was employed to estimate the directional spectrum because of its high versatility and relatively high accuracy.

Using polar coordinates (**Fig. 4**), the water particle velocity  $U$  in the direction  $r$  with coordinates  $(\alpha, \beta, r)$  is obtained by

$$U(\alpha, \beta, r, h, z_0; \omega, \theta) = H(\alpha, \beta, r, h, z_0; \omega, \theta) \eta(\alpha, \beta, r; \omega, \theta), \quad (6)$$

where  $\eta$  is the water surface elevation and  $H$  the transfer function between  $U$  and  $\eta$ .  $H$  can be expressed using linear wave theory as follows:

$$H(\alpha, \beta, r, h, z_0; \omega, \theta)$$

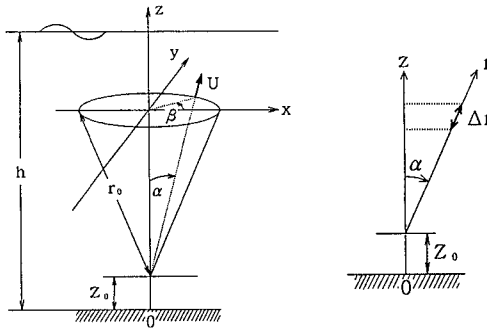


Fig. 4 Definition of polar coordinates.

$$\begin{aligned}
 &= \frac{\omega}{\sinh kh} \left[ \cosh\{k(r \cos \alpha + z_0)\} \right. \\
 &\quad \times \sin \alpha \cos(\theta - \beta) \\
 &\quad \left. - i \sinh\{k(r \cos \alpha + z_0)\} \cos \alpha \right], \tag{7}
 \end{aligned}$$

where  $h$ ,  $k$ ,  $\omega$ ,  $\theta$ , and  $z_0$  respectively represent the water depth, wave number, angular frequency, wave propagation direction, and height at which the meter is installed above the seabed.

When the water surface elevation  $\eta_0$  above the origin  $(0,0,0)$  is used as a basis, the transfer function between  $U$  and  $\eta_0$  is obtained by multiplying Eq. (7) by  $\exp[i\{kr \sin \alpha \cos(\theta - \beta) - \omega \Delta t\}]$ , i.e.,

$$\begin{aligned}
 &H_0(\alpha, \beta, r, h, z_0; \omega, \theta) \\
 &= \frac{\omega \exp(-i\omega \Delta t)}{\sinh kh} \left[ \cosh\{k(r \cos \alpha + z_0)\} \right. \\
 &\quad \times \sin \alpha \cos(\theta - \beta) - i \sinh\{k(r \cos \alpha + z_0)\} \\
 &\quad \left. \times \cos \alpha \right] \exp\{ikr \sin \alpha \cos(\theta - \beta)\}, \tag{8}
 \end{aligned}$$

where  $\Delta t$  is the time lag between the measurement of each velocity component and that of  $\eta_0$ .

The current velocity component detected by a Doppler-type wave meter is not the water particle velocity at a specified location, but instead an average velocity in a volume of known width  $\Delta r$ . Therefore, by disregarding the width around the  $r$  axis

and integrating Eq. (8) in terms of  $r$ , the transfer function between  $U$  in the direction  $r$  with coordinates  $(\alpha, \beta, r)$  and  $\eta_0$  above the origin  $(0,0,0)$  is represented as:

$$\begin{aligned} \bar{H}(\alpha, \beta, r_0, \Delta r, z_0, \omega, \theta) &= \frac{1}{\Delta r} \int_{r_0 - \Delta r/2}^{r_0 + \Delta r/2} H_0(\alpha, \beta, r, h, z_0, \omega, \theta) dr \\ &= \frac{-i\omega \exp(-i\omega\Delta t)}{\Delta r k \sinh kh} \left[ \cosh\{k(r \cos \alpha + z_0)\} \right. \\ &\quad \left. \times \exp\{ikr \sin \alpha \cos(\theta - \beta)\} \right]_{r_0 - \Delta r/2}^{r_0 + \Delta r/2} \end{aligned} \quad (9)$$

Employing Eq. (9) leads to the estimation equation of the directional spectrum by the EMLM, i.e.,

$$S(f, \theta) = \frac{\kappa}{\mathbf{H}^* \Phi^{-1} \mathbf{H}}, \quad (10)$$

where  $\mathbf{H}$  is the matrix comprised of the transfer functions given by Eq. (9),  $\mathbf{H}^*$  the complex conjugate of the transpose matrix of  $\mathbf{H}$ ,  $\Phi^{-1}$  the inverse matrix of matrix  $\Phi$  consisting of the cross-power spectra between each quantity, and  $\kappa$  is a proportionality constant used to normalize the energy of the directional spectrum.

### 3. Field observations

Field observations were carried out off the entrance of Kamaishi Bay (Fig. 5) after installing the transducer 0.95 m above the seabed at a water depth of 35 m. The

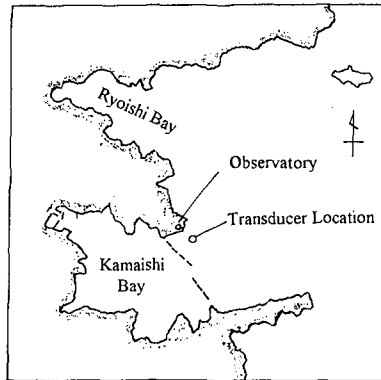


Fig. 5 Field observation location.

**Table 2** Sea conditions during the field observations.

Obs. No.	Date	Runs	Wave height (m)	Wave period (s)	Water depth (m)	Depth of scattered layer $Z_u$ (m)
1	Aug.'90	12	0.69~1.51	9.8~10.6	34.51~35.6	3.56 - 9.90
2	Nov.'90	44	0.32~1.00	6.3~13.3	34.94~36.12	8.99 - 10.17
3	Dec.'90	20	1.16~1.88	9.3~12.7	35.08~36.32	9.13 - 10.37
4	Mar.'91	44	0.76~1.84	5.6~10.6	35.56~36.46	9.01 - 10.51

measured signals were transmitted via a submarine cable to a land-based observatory (Miyako Port Construction Office, 2nd District Port Construction Bureau, Ministry of Transport). The water surface elevation ( $Z$ ) and four current velocity components ( $X^+$ ,  $X^-$ ,  $Y^+$ ,  $Y^-$ ) were recorded on an optical magnetic disk at a 0.99-s sampling interval. **Table 2** summarizes the sea conditions during the field observations.

The current velocities were measured 25 m above the transducer, with the thickness  $\Delta r$  of the scattering layers being about 2.3 m.  $\alpha$  was set at  $30^\circ$  (**Fig. 1**). We assumed a constant sound velocity of 1500 m/s for the computation.

3.1 Validity of the transfer function

The validity of the Eq. (9) transfer function cannot be directly verified using the observed data. However, by linear wave theory, the value  $\{\text{Re}(\bar{H})\}^2 + 2\{\text{Im}(\bar{H})\}^2$  can be approximated by dividing the sum of the power spectrum of water particle

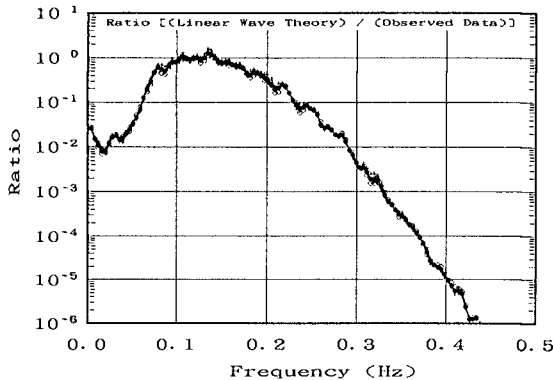


**Fig. 6** Validity of transfer function



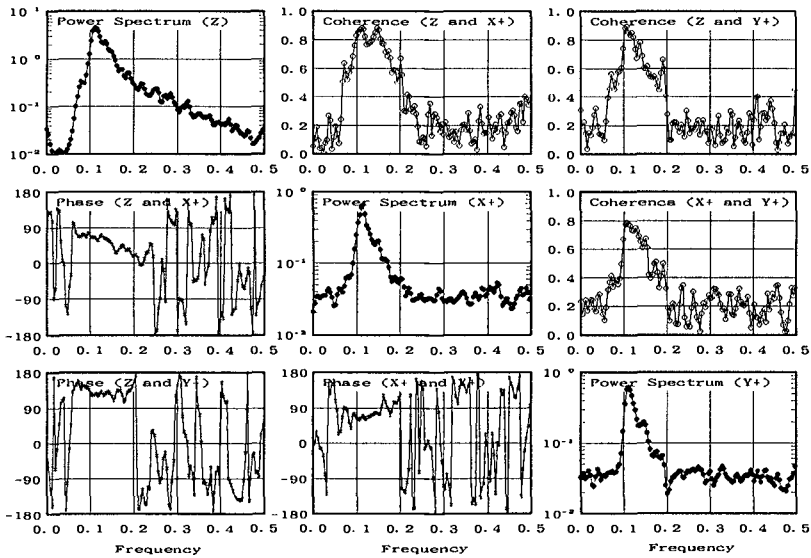


Fig. 7 Typical results of cross-power spectra estimations.

velocities in the X- and Y-directions by the power spectrum of the water surface elevation. **Figure 6** shows this ratio, which is near 1.0 from 0.08 to 0.15 Hz; hence, Eq. (9) can be considered as being valid.

### 3.2 Estimation of directional spectrum

Typical cross-power spectra estimated from the observed data are shown in **Fig. 7**, where the coherence between each wave quantity is high near the peak frequency of the power spectra and the phase angle shows continuous, smooth fluctuations from 0.06 to 0.2 Hz. These results indicate the field observation cross-power spectra are reasonable.

**Figure 8** shows typical directional spectra estimated by the EMLM, where various combinations of quantities are indicated since the EMLM enables using a data set consisting of three or more quantities. The entrance of Kamaishi Bay faces east, and all these results clearly show that waves come from the appropriate direction.

In addition, a reasonable directional spectrum was estimated in 99 out of 122 observations. Of the 23 observations from which adequate results were not estimated, 16 had water surface elevation contaminated by the noise, while the remaining 7 contained erroneous measurements.

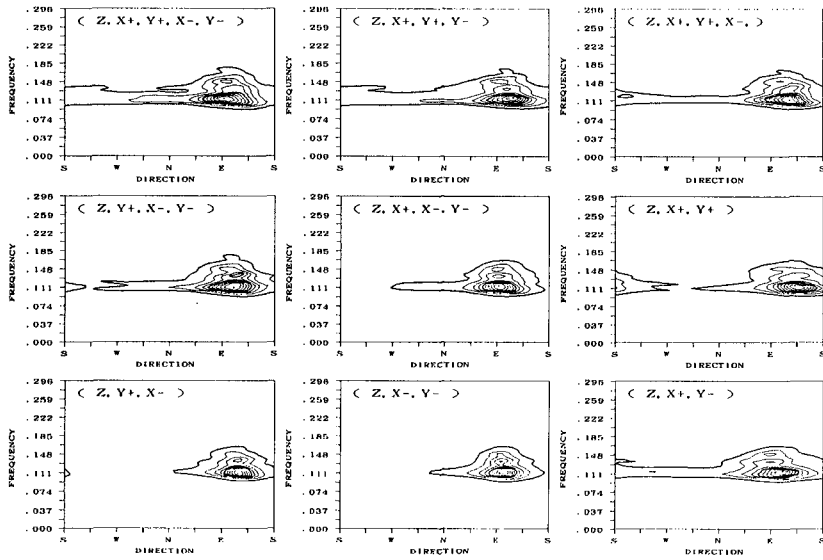


**Fig. 8** Typical directional spectra estimated using various combinations of quantities.

In cases where reasonable results were obtained, for  $z_U$  from 9 to 10 m, a measurement was obtained even when the significant wave height was only 35 cm at a significant wave period of about 10 s. Furthermore, at a significant wave period of about 6 s, waves with a significant wave height of 1 m were measured. It should be realized that the highest significant wave height for these observations was 1.85 m, which is not a severe sea condition. Under more severe sea conditions, however, measurement is believed to be possible by increasing  $z_U$ .

#### 4. Conclusions

Knowledge of directional spectra is essential for clarifying various coastal engineering problems. However, difficulties in measuring directional seas have led to insufficient information being available. Since the submerged Doppler-type directional wave meter can be employed to measure directional seas with only one set of units and provide an accurate estimation of directional spectrum. It is considered to be the best measuring system for investigation and research on directional seas. In fact, in the near future, Japan's Nationwide Ocean Wave information network for Ports and HARbourS (NOWPHAS) (Nagai et al., 1993) will install this instrument at all their coastal wave observation stations.

### Acknowledgments

This research was jointly carried out by the Port and Harbour Research Institute, Ministry of Transport, and Japan Marine Surveyors Association under the direction of the Committee for the Development of a Submerged Doppler-Type Directional Wave Meter (Chairman, Professor Y. Goda, Yokohama National University) organized by the Japan Marine Surveyors Association. The analyzed field wave data were contributed by the Second Port Construction Bureau, Ministry of Transport. Sincere gratitude is extended to all those involved in this study.

### References

- Isobe, M., K. Kondo and K. Horikawa (1984): Extension of MLM for estimating directional wave spectrum, Proc. Symp. on Description and Modeling of Directional Seas, Paper No. A-6, 15 p.
- Ito, Y., Y. Kobori, M. Horiguchi, M. Takehisa and Y. Mituta (1989): Development of Wind Profiling Sodar, J. Atmos. Oceanic Tech., Vol. 6, pp.779-784.
- Nagai, T., K. Sugahara, N. Hashimoto and T. Asai (1993): 20-year statistics of the Nationwide Ocean Wave information network for Ports and HARbourS (NOWPHAS 1970-1989), Tech. Note of Port and Harbour Res. Inst., No. 744, 247 p.
- Nagai, T., K. Sugahara, N. Hashimoto and T. Asai (1993): Annual Report on the Nationwide Ocean Wave information network for Ports and HARbourS (NOWPHAS 1991), Tech. Note of Port and Harbour Res. Inst., No. 745, 304 p.